The 14th IFToMM World Congress, Taipei, Taiwan, October 25-30, 2015
DOI Number: 10.6567/IFToMM.14TH.WC.OS13.024

Robustness Improvement of Trajectory Planning Algorithms

P. Boscariol
DIEGM
University of Udine, Italy

R. Vidoni
Faculty of Science and Technology
Free University of Bolzano, Italy

A. Gasparetto*
DIEGM
University of Udine, Italy

Abstract—*In this paper the topic of robust model based trajectory planning for mechatronic systems is dealt with. The aim is to improve, using sensitivity techniques, the robustness to parametric mismatches of commonly used indirect variational methods. The necessary optimality conditions are derived using Pontryagin's minimum principle, and the robustness condition are obtained by imposing boundary constraints on sensitivity functions. Unlike other methods available in literature, the proposed method can be applied to nonlinear models. Several test cases are reported to show the unconstrained and the constrained solution for nonlinear mechatronic systems.*

Keywords: trajectory planning, robust, nonlinear system

I. Introduction

High speed and high efficiency robotics cannot be achieved without the use of clever closed-loop control system and smooth trajectory planning. This factors are even more important if the robot presents some sort of structural flexibility, since the presence of oscillations even after the completion of the task can severely reduce the operativeness of the robot [1], [2], [3]. This flexibility, which might be due to the joint [4] or link [5], [6] mechanical structure, is the source of several challenging problems. Extensive research have been developed to find a solution to the problem of vibration phenomena through the generation of suitable trajectories, as reported in the review papers [7], [8]. In this sense, a main distinction can be made among model-based and model-free approaches. The advantage of the first method is that the results can be easily adapted to several robots, and that the results are independent from the knowledge of the accurate dynamics of the robot. On the other hand, this kind of approach can potentially lead to high level of performance, even for high complexity models [9], [10]. The majority of this works are based on optimal control theory, and therefore they often limited in their robustness properties, as highlighted in [11]. In this means that a trajectory that is optimal in the nominal case, can be disadvantageous in if applied to a perturbed plant.

Most model-free approaches are based on geometrical approaches, i.e. the trajectory is based on the composition of polynomial functions [12], [13], splines [8] or nurbs [14]. Generally this approaches are targeted at maximizing the smoothness of the trajectory by obtaining continuous and low peak values of jerk [15].

Model-based approach have been studied in a large number of works, with applications to basically every kind of robot. The solution of the planning problem has been investigated for mobile robots in papers such as [16]. Flexible joint robot have been considered in [17], [18]. Also the design of trajectories for Flexible-Link Manipulators (FLM) have been studied quite extensively [19]. Approaches based on the definition and the solution of Two-Point Boundary Value Problems (TPBVP) have been developed, among others, in [20], [9]. In these works a point-to-point trajectory is computed by solving a constrained optimization problem, by imposing that the trajectory must connect the two boundary points while respecting the robot dynamics.

In this work a solution to the problem of computation of constrained point-to-point trajectories is analyzed using TPBVP techniques, but with a particular focus on the robustness of the solution to parametric uncertainties. The topic of robustness have been extensively studied in the area of closed-loop control. The literature on the topic is very extensive, but to the best of authors' knowledge, there are very few works that specifically focus on robust trajectory planning algorithms.

One example is [21], in which robustness is achieved by introducing in the fitness function a term of Gaussian cumulative noise. The work by Shin [22] focuses on the definition of robot trajectories by taking into account the uncertainties brought by payload variations through the change of bounds on joint torques. Other interesting approaches to robust trajectory planning are currently available as solutions to the problem of robust optimization for dynamic systems: an extensive overview of this problem is available in [23].

The aim of this paper is to propose a method for planning a trajectory which is based on two-point boundary value problems and on the concept of desensitization. Sensitivity function have been used in [24], [25], [26] to improve the robustness of closed-loop optimal controllers. The design of such controllers is done analytically, since a solution of this kind can be found is the plant taken into consideration is linear. It must be highlighted that the method proposed here applies to nonlinear plants, therefore it greatly enhances the field of application of the method presented in [24], [25], [26].

The inclusion of constraints on actuator action also plays an important role in most real-world applications, in which

*alessandro.gasparetto@uniud.it

the actuator's capabilities must be exploited up to their full potential and without violating the actuator's safe operating area. Among the techniques presented in the papers [24], [25], [26],the only one that allows to include constraints is [26], but the method used to limit the control action in that paper cannot be directly applied to the class of problems considered in this work.

The outcome of the approach presented in this paper is a position profile for the system to be operated that can be used by most industrial PLC-based controller.

II. Variational solution of the trajectory planning problem

The target here is to develop an optimal trajectory for a mechatronic system. We consider here point-to-point trajectory optimization problems, in which only the initial and final end-effector positions are given, and the manipulator is free to move between them. Therefore both the path and the trajectory are subject to optimization, and they are selected with the aim of minimizing a cost functional. Such cost may depend on execution time, actuator effort, jerks (or torque rates), or a combination of these variables. First of all, let us define the optimization problem that we want to solve. Given a dynamic system, that might be linear or nonlinear, described by a set of differential equation in the form:

$$\dot{\mathbf{x}} = \Omega(\mathbf{x}, t, \mathbf{u}) \tag{1}$$

in which $\mathbf{x}$ is the vector of state variables of the system, and $\mathbf{u}$ is the control vector. If we choose a cost function:

$$J = f(\mathbf{x}, t, \mathbf{u}) \tag{2}$$

the following optimization problem can be stated:

$$\begin{cases} \min J(\mathbf{x}(t), t, \mathbf{u}) = \min \int_{t_0}^{t_f} f(\mathbf{x}, t, \mathbf{u}) dt \\ s.to. \\ \mathbf{x}(t_0) = \alpha \\ \mathbf{x}(t_f) = \beta \\ \dot{\mathbf{x}}(t) = \Omega(\mathbf{x}(t), t, \mathbf{u}) \end{cases} \tag{3}$$

in which α and β are some constant vector of the same size of $\mathbf{x}$ used to define the initial and final conditions for the dynamic system. The solution of this optimization problems allows to find the trajectory for the state vector $\mathbf{x}$ that minimizes the cost function J. The trajectory is constrained to respect the dynamics of the system $\Omega(\mathbf{x}, t, u)$ and the value of $\mathbf{x}$ at the initial ($t = t_0$) and final ($t = t_f$) time. A solution of the optimization problem in equation (3) can be found using the calculus of variations and Pontryagin's Minimum Principle (PMP) [27].

First of all, the Hamiltonian of the system must be defined as:

$$\mathcal{H} = f(\mathbf{x}, t, \mathbf{u}) + \boldsymbol{\lambda}(t)^T \Omega(\mathbf{x}(t), t, \mathbf{u}) \tag{4}$$

in which $\boldsymbol{\lambda}(t) = [\lambda_1(t), \ldots, \lambda_N(t)]^T$ is the vector of Lagrangian multipliers, called also costate vector, which has the same size of the state vector $\mathbf{x}$. The necessary conditions for finding a minimum of the problem in Eq. (3) are, according to the PMP:

$$\frac{\partial \mathcal{H}}{\partial \mathbf{u}} = 0 \tag{5}$$

$$\dot{\mathbf{x}} = \frac{\partial \mathcal{H}}{\partial \boldsymbol{\lambda}} \tag{6}$$

$$\dot{\boldsymbol{\lambda}} = -\frac{\partial \mathcal{H}}{\partial \mathbf{x}} \tag{7}$$

The above conditions can be put in a single system that makes the computation straightforward. By defining $\mathbf{u}^*$ the solution of equation (5), $\mathcal{H}^*(\mathbf{x}, t, \boldsymbol{\lambda})$ is the Hamiltonian in which $\mathbf{u}$ has been substituted with $\mathbf{u}^*$. $\mathcal{H}^*$ is called the minimizing Hamiltonian. A new system of ordinary differential equation can be defined as:

$$\dot{\mathbf{y}} = \begin{bmatrix} \dfrac{\partial \mathcal{H}^*}{\partial \boldsymbol{\lambda}} \\ -\dfrac{\partial \mathcal{H}^*}{\partial \mathbf{x}} \end{bmatrix} \tag{8}$$

The new state vector $\mathbf{y}$ is obtained by augmenting the original state vector $\mathbf{x}$ with the vector of Lagrangian multipliers:

$$\mathbf{y} = \begin{bmatrix} \mathbf{x} \\ \boldsymbol{\lambda} \end{bmatrix} \tag{9}$$

Among the infinite possible trajectories of the dynamic system in equation (1), we are interested in finding the one that obeys to the boundary conditions $\mathbf{x}(t_0) = \alpha$ and $\mathbf{x}(t_f) = \beta$.

A solution to this problem, that is basically a TPBVP (Two-Point Boundary Value Problem), could theoretically be found in closed form. In many cases, however, it is solved numerically, given the difficulty of finding an analytic solution. Collocation method [9], [28] and shooting method [29] are often used for this task.

A. Robustness improvements with sensitivity functions

The problem presented and solved in the previous section works very well when the dynamic model used for planning the trajectory can reproduce faithfully the actual dynamics of the real system. This does not happen in all situations, given the difficulty of describing a complex plant with a reasonably simple model. Moreover, sometimes it is not even possible to describe the dynamics of the plant with just a single model. A common situation is when a robot is driving a payload that changes, as in a pick & place operation. As the mass carried by the robotic manipulator changes, also its dynamic model is altered. Quite often also nonlinearities might be neglected during the modeling phase: in

this case the trajectory planning algorithm and the control loop are required to compensate for the model-plant mismatches.

The main idea behind the technique used in this paper is to augment the plant dynamic model with the partial derivatives of the ODE (Ordinary Differential Equation) system with respect to a parameter η of choice. These partial derivatives are called sensitivity functions. By imposing that their values must be zero at a given point of a trajectory, the robustness with respect to the parameter η is increased. The effectiveness of this approach has been shown both numerically [25], [24], and experimentally [26] but only for the design of closed-loop control strategies for linear systems. For this reason the procedure followed in the aforementioned papers cannot be applied to the test cases used here, which involve nonlinear systems.

The procedure used to solve the robust optimization problem starts form an augmentation of the system of ordinary differential equations $\Omega(\mathbf{x}, t, \eta)$ that describe the dynamics of the plant under consideration, which is also influenced by a parameter η.

If $\Omega(\mathbf{x}, t, \eta)$ has continuous first partial derivatives with respect to η and $\mathbf{x}$, and η_0 is the nominal value of η, the time evolution of $\mathbf{x}(t)$ from the initial state $\mathbf{x}_0$ can be evaluated as:

$$\mathbf{x}(t, \eta) = \mathbf{x}_0 + \int_{t_0}^{t} \Omega(s, \mathbf{x}(s), \eta) ds \tag{10}$$

The partial derivatives of the latter with respect to the parameter η are:

$$\mathbf{x}_\eta(t, \eta) = \int_{t_0}^{t} \frac{\partial \Omega(s, \mathbf{x}(s, \eta), \mathbf{x}_\eta)}{\partial x} + \frac{\Omega(s, \mathbf{x}(s, \eta), \eta)}{\partial \eta} ds \tag{11}$$

in which $\mathbf{x}_\eta = \dfrac{\partial \mathbf{x}(t, \eta)}{\partial \eta}$ and $\dfrac{\partial \mathbf{x}_0}{\partial \eta} = 0$. The partial derivatives of eq. (11) with respect to time can be therefore written in the form:

$$\frac{\partial \mathbf{x}_\eta(t, \eta)}{\partial t} = \mathbf{A}(t, \eta)\mathbf{x}_\eta(t, \eta) + \mathbf{B}(t, \eta) \tag{12}$$

in which:

$$\mathbf{A}(t, \eta) = \left.\frac{\partial \Omega(\mathbf{x}, t, \eta)}{\partial \mathbf{x}}\right|_{\mathbf{x}=\mathbf{x}(t,\eta)}; \mathbf{B}(t, \eta) = \left.\frac{\partial \Omega(\mathbf{x}, t, \eta)}{\partial \eta}\right|_{\mathbf{x}=\mathbf{x}(t,\eta)}$$

Now, using the definition $\mathbf{S}(t) := \mathbf{x}_\eta(t)$, eq. (12) can be rewritten as:

$$\dot{\mathbf{S}}(t) = \mathbf{A}(t, \eta)\mathbf{S}(t) + \mathbf{B}(t, \eta) \tag{13}$$

$\mathbf{S}(t)$, i.e. the solution of eq. (13) is the vector of sensitivity functions of the ODE system $\Omega(\mathbf{x}, t, \eta)$, i.e. the functions used to evaluate the effect of a variation of the value of parameter η on the dynamics of the system. Now an augmented system of differential equations can be composed by joining equation (1) with the system in equation (13):

$$\begin{bmatrix} \dot{\mathbf{x}}(t) \\ \dot{\mathbf{S}}(t) \end{bmatrix} = \begin{bmatrix} \Omega(\mathbf{x}(t), t, \mathbf{u}, \eta) \\ \mathbf{A}(t, \eta)\mathbf{S}(t, \eta) + \mathbf{B}(t, \eta) \end{bmatrix} \tag{14}$$

It should be highlighted that the definition of the sensitivity equations allows to calculate in a straightforward manner eq. (14), since:

$$\begin{aligned} \mathbf{S}(t) := \frac{\partial \mathbf{x}(t)}{\partial \eta}; \quad \dot{\mathbf{S}}(t) = \frac{d}{dt}\frac{\partial \mathbf{x}(t)}{\partial \eta}; \\ \mathbf{A}(t, \eta)\mathbf{S}(t, \eta) + \mathbf{B}(t, \eta) = \frac{\partial \Omega(\mathbf{x}(t), t, \mathbf{u})}{\partial \eta} \end{aligned} \tag{15}$$

In the cases under consideration here the uncertain parameter is just one, η, but the method shown here allows to take into consideration an arbitrary number of uncertain parameters. If $\mathbf{x}(t) \in \Re^n$, and there are m uncertain parameters, than simply $\mathbf{S}(t) \in \Re^{nm}$.

Now the optimization problem in equation (3) can be reformulated by including the sensitivity conditions as well:

$$\begin{cases} \min J(\mathbf{x}(t), \mathbf{S}(t), t, \mathbf{u}) = \min \int_{t_0}^{t_f} f(\mathbf{x}, \mathbf{S}, t, \mathbf{u}) dt \\ s.to. \\ \mathbf{x}(t_0) = \alpha \\ \mathbf{x}(t_f) = \beta \\ \mathbf{S}(t_0) = 0 \\ \mathbf{S}(t_f) = 0 \\ \dot{\mathbf{x}}(t) = \Omega(\mathbf{x}(t), t, \mathbf{u}) \\ \dot{\mathbf{S}}(t) = \mathbf{A}(t, \eta)\mathbf{S}(t, \eta) + \mathbf{B}(t, \eta) \end{cases} \tag{16}$$

The difference between equation (3) and (16) is that the latter problems include a larger number of constraints. As it will be shown in the following, by imposing that the sensitivity function are equal to zero at the beginning and at the end of the trajectory, the parametric robustness of the planned trajectory can be improved.

Here parametric robustness is intended as the robustness of the solution with respect to a deviation of an uncertain parameter of the plant from its nominal value. Two different metrics are used to quantify the parametric robustness: in section III the metric is the maximum amplitude of residual vibration, while for the test case included in section IV the metric is the residual energy of the system.

A brief outline of the procedure to be followed to synthesize a robust trajectory can be:

1. Define the dynamics of the plant
2. Define the uncertain parameter and the sensitivity functions according to eq. (15)
3. Define augmented dynamics of the system with sensitivity functions

4. Compute the Hamiltionian of the augmented system according to eq. (8)
5. Define the boundary conditions
6. Solve numerically the optimization problem in eq. (16)

III. Numerical results: unconstrained solution

In order to show the effectiveness of the robust approach by the use of sensitivity functions, a simple test case is taken into consideration. The mechanic system is a single mass system coupled to a rigid structure by a nonlinear spring, as in Figure 1. This system is chosen to represent the class of systems with low-frequency nonlinear oscillators, like gantry cranes [30], tape drives or tanks with slosh. The nonlinearity of the system is due to the nonlinear elastic force exerted by the spring, which is:

$$F = kq + kq^3 \tag{17}$$

being $q(t)$ the displacement of the mass from the rest position and k is the elastic constant of the pring. If $u(t)$ is the external force applied to the mass, the differential equation that describes the dynamics of the system is the second-order differential equation:

$$m\ddot{q} = -kq - kq^3 + u \tag{18}$$

The second-order ODE in equation (18) can be written in its first-order version by choosing the state vector $\mathbf{x}$ as $\mathbf{x} = [\dot{q}, q]^T$. With this choice the ODE system that will be used to compute the optimal trajectory is:

$$\dot{\mathbf{x}} = \begin{bmatrix} -\dfrac{k}{m}(q+q^3) + \dfrac{u}{m} \\ \dot{q} \end{bmatrix} \tag{19}$$

The system in eq. (19) can be augmented by including the two sensitivity function of the state vector $\mathbf{x}$ with respect to the elastic constant k, according to the notation of equation 14:

$$\begin{aligned} \frac{d}{dt}\left(\frac{\partial \dot{q}}{\partial k}\right) &= -\frac{1}{m}(q+q^3) - \frac{k}{m}\frac{\partial q}{\partial k}\left(1+3q^2\right) \\ \frac{d}{dt}\left(\frac{\partial q}{\partial k}\right) &= \frac{\partial \dot{q}}{\partial k} \end{aligned} \tag{20}$$

In this formulation the vector of sensitivity functions is $\mathbf{S}(t) = \left[\dfrac{\partial \dot{q}}{\partial k}, \dfrac{\partial q}{\partial k}\right]^T$. Therefore the TPBVP must be formulated considering as the plant dynamics the augmented ODE:

$$\begin{bmatrix} \dot{\mathbf{x}}(t) \\ \dot{\mathbf{S}}(t) \end{bmatrix} = \begin{bmatrix} -\dfrac{k}{m}(q+q^3) + \dfrac{u}{m} \\ \dot{q} \\ -\dfrac{1}{m}(q+q^3) - \dfrac{k}{m}\dfrac{\partial q}{\partial k}\left(1+3q^2\right) \\ \dfrac{\partial \dot{q}}{\partial k} \end{bmatrix} \tag{21}$$

Now the number of ODE is four, therefore the application of the PMP requires to use four Lagrangian multipliers. The solution of the optimization problem in the nominal and robust cases leads to the definition of the trajectories shown in figure 3. The boundary conditions chosen are: $\dot{q}(0) = \dot{q}(t_f) = 0$, $q(0) = 1$ and $q(t_f) = 0$. Therefore a rest-to-rest motion is implemented. The force profile $u(t)$, shown in figure 2 computed together with the solution of the optimization problem has been applied to two perturbed plants, having values of the spring stiffness equal to $k = 1.4\ N/m$ and $k = 0.6\ N/m$, therefore in the cases of a parametric mismatch equal to $\pm 40\%$. This test allows to evaluate the robustness of the computed trajectories. The response of the system with $k = 1.4\ N/m$ is shown in fig. 4. It can be clearly seen that in that case the residual vibration, i.e. the mass displacement after 2 seconds is notably larger in the non-robust case than in the robust case. An ever smaller residual vibration is obtained in the case depicted in figure 5: the vibration amplitude after the task completion is almost equal to zero.

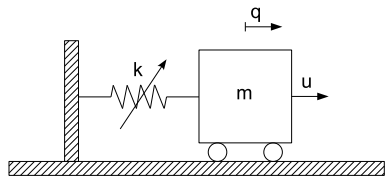

Fig. 1. Testbench I: nonlinear oscillator

A more complete comparison in terms of residual vibration is shown in figure 6, in which the peak amplitude of residual vibration are shown for a range of perturbation equal to $\pm 70\%$. According to the works [24], [25], [26], the maximum amplitude of residual vibration are used as a measurement of the robustness of the proposed approach. It can be seen in figure 6 that the robust trajectory allows a sensible reduction of residual vibration for all the cases taken into consideration. Moreover, null residual vibration is preserved for the nominal value of k by the robust trajectory. The only drawback of the proposed approach is the larger actuation force requirement, as it can be seen in figure 2.

IV. Numerical results: constrained solution

As mentioned in the previous section, the robust solution can have the drawback of requiring a larger force require-

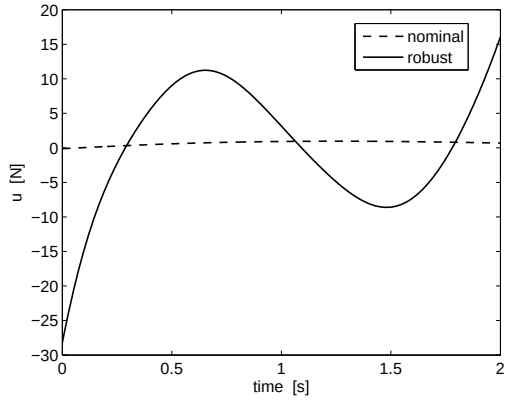

Fig. 2. Mass-spring system: nominal and robust control action

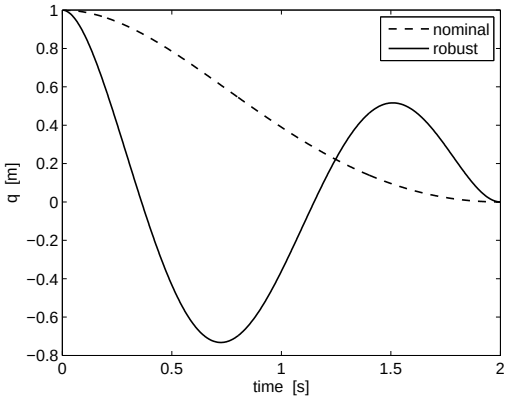

Fig. 3. Nominal and robust trajectory for nonlinear spring-mass system: mass position q

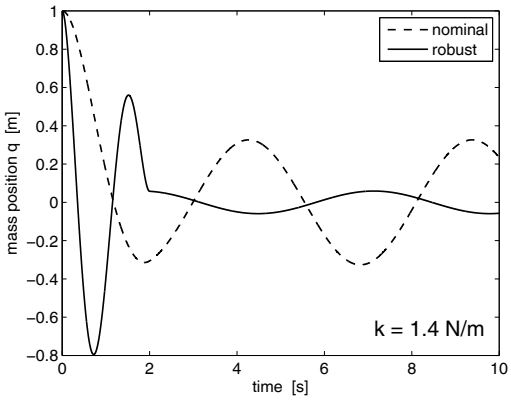

Fig. 4. Response of the system with $k = 1.4$ N/m: nominal and robust trajectories

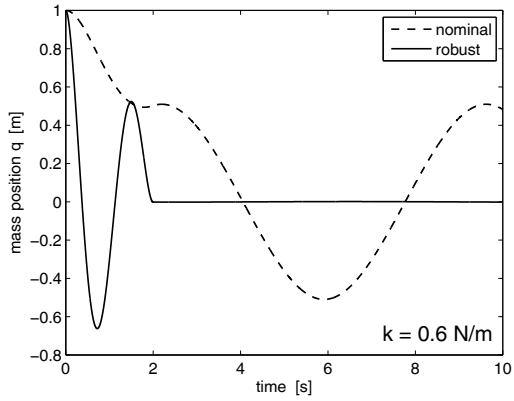

Fig. 5. Response of the system with $k = 0.6$ N/m: nominal and robust trajectories

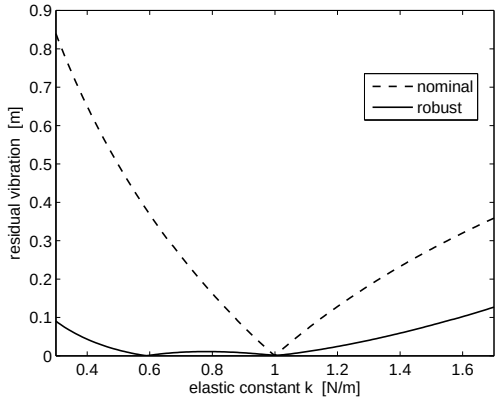

Fig. 6. Peak residual vibration vibration with $k \in [0.3, 1.7]\ N/m$: comparison between nominal and robust trajectories

ment. This disadvantage can be compensated through the inclusion of constraints in the solution of the optimization problem. The method used to introduce constraints will be shown here through another testbench problem. The structure of the mechanism is shown in figure 7. The system reproduced an elastic joint of a robot with a nonlinear spring characteristic. If Δq is the relative angular displacement of the two inertias J_1 and J_2, the force excerpted by the torsional spring is:

$$F(\Delta q) = k(\Delta q + \Delta q^3) \tag{22}$$

This kind of model can be used to model a single joint of

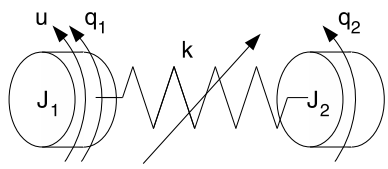

Fig. 7. Testbench II: Nonlinear flexible joint

an industrial robot with elasticity, as reported in the works [31], [32], [33]. Such model has also been used to reproduce the dynamics of an ABB IRB6600 industrial robot in [4]. The dynamics of the system is:

$$\begin{aligned} J_1\ddot{q}_1 &= k(q_2-q_1)+k(q_2-q_1)^3+u \\ J_2\ddot{q}_2 &= -k(q_2-q_1)-k(q_2-q_1)^3 \end{aligned} \tag{23}$$

in which u is the motor torque applied to the first mass of inertia J_1, while the second mass has inertia J_2. The speed of rotation of the mass will be indicated as $\dot{q}_1$ or ω_1 for the first mass and $\dot{q}_2$ or ω_2 for the second mass. If $J_1 = J_2 = 1$, the dynamics of the system in eq. 23 can be rewritten as:

$$\dot{\mathbf{x}} = \begin{bmatrix} k(q_2-q_1)+k(q_2-q_1)^3+u \\ -k(q_2-q_1)-k(q_2-q_1) \\ \omega_1 \\ \omega_2 \end{bmatrix} \tag{24}$$

The procedure shown in section 2 cannot be directly applied in this case if constraints are to included in the problem. This is due to the fact that the application of Pontryagin's minimum principle requires for the Hamltionian to be differentiable in time with continuous derivatives in $\mathbf{x}(t)$ and $\Lambda(t)$, and therefore hard constraints cannot be applied using a saturation function. The proposed solution to this situation is the use of a smoothing function.

First, let us take into consideration the nominal solution of the trajectory planning problem without constraints. The Hamiltonian of the systems for the minimum effort solution is:

$$\begin{aligned} \mathcal{H} = \lambda_3\omega_1 - \lambda_1(k(q_1-q_2)-u+k(q_1-q_2)^3) \\ +\lambda_4\omega_2 + \lambda_2(k(q_1-q_2)+k(q_1-q_2)^3)+\frac{u^2}{2} \end{aligned} \tag{25}$$

and the application of the condition in eq. (5) leads to:

$$\frac{\partial \mathcal{H}}{\partial u} = u + \lambda_1 \tag{26}$$

The last equation highlights that the optimal control action is $u^* = -\lambda_1$, therefore the system of ordinary differential equations to be solved is:

$$\dot{\mathbf{y}}^* = \begin{bmatrix} -\lambda_1 - k(q_1-q_2)-k(q_1-q_2)^3 \\ k(q_1-q_2)+k(q_1-q_2)^3 \\ \omega_1 \\ \omega_2 \\ -\lambda_3 \\ -\lambda_4 \\ k(\lambda_1-\lambda_2)(3{q_1}^2-6q_1q_2+3{q_2}^2+1) \\ -k(\lambda_1-\lambda_2)(3{q_1}^2-6q_1q_2+3{q_2}^2+1) \end{bmatrix} \tag{27}$$

The problem defined in the last equation is unconstrained. A simple solution can be found to constrain one or more of the state and lagrangians through the use of a smooth saturation function. The definition of the saturation function is:

$$sat(s,\gamma) = \begin{cases} s, & |s| < \gamma \\ \gamma sign(s), & |s| > \gamma \end{cases} \tag{28}$$

which can be approximated as:

$$SAT(s,\gamma,\nu) = \frac{\gamma}{2}\left(\sqrt{\nu+\left(\frac{s}{\gamma}+1\right)^2} - \sqrt{\nu+\left(\frac{s}{\gamma}-1\right)^2}\right) \tag{29}$$

This approximation has been introduced and used by Avvakumov in [34] for the constrained solution of boundary value problem. The quality of the approximation is inversely proportional to the constant positive parameter ν. Simple numerical evaluations show that a sufficiently good approximation can be achieved for $\nu = 1e-6$: for this value of ν the approximation error, i.e. the difference between the ideal saturation function and its approximating function, is less than $2e-4$ for $\gamma = 1$. The application of this approximated saturation function to the problem stated in eq. (27) requires simply to substitute in it λ_1 with the expression in eq. (29). This allows to limit λ_1, and therefore u^*, in the range $u \in [-\gamma, \gamma]$.

In the following the results of the computation of the trajectory planning algorithm are shown. The boundary conditions are set in order to bring the two masses from the initial position $q_1(t=0) = 0.1$ rad and $q_2(t=0) = 0.1$ rad to $q_1(t=t_f) = q_2(t=t_f) = 0$ rad with initial and final speed equal to zero. Therefore a rest-to-rest motion is planned. In this case the total execution time is chosen to be $t_f = 2$ s. The values of u is limited in the range $[-2.5, 2.5]$ Nm for the constrained solution.

The control action u is for the unconstrained and constrained case is shown in figure 8. The planned trajectory is shown in Fig. 9. In particular, it can be seen that the inclusion of constraints allows to precisely limit the amplitude of u: as imposed in the definition of the optimization problem, the torque provided by the motor never exceeds the prescribed value of 2.5 Nm. This result has been obtained with $\nu = 1 \times 10^{-9}$. It has been verified numerically that lowering the value of ν does not improve the quality of the solution. The actual trajectories for the unconstrained and constrained solutions are similar to each other, as it can be seen in Figure 5. In the constrained case the first mass achieves a slightly higher speed than in the nominal case, which is a direct effect of the torque limitation.

The application of the control profile $u(t)$ shown in figure 8 to a nominal plant, i.e. to a plant in which the spring stiffness is proportional to $k = 1\ Nm/rad$ is shown in figure 10, which shows that zero residual vibration can be achieved also in the presence of constraints.

On the other hand if a perturbed plant is taken into consideration, and in particular if the value of k is increased by 30%, the application of the feedforward torque profile

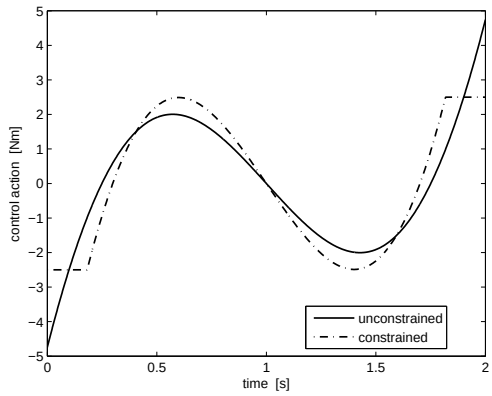

Fig. 8. Control action for the nominal case: constrained and unconstrained solutions

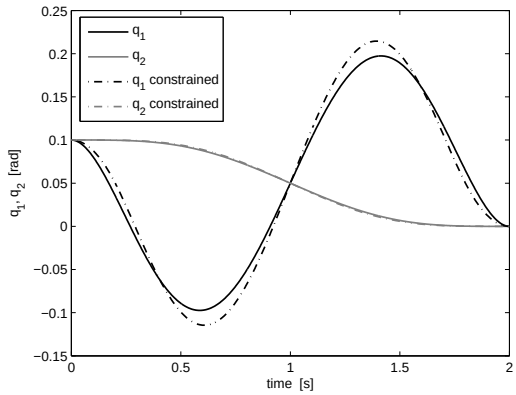

Fig. 9. Joint trajectory for the nominal case: constrained and unconstrained solution

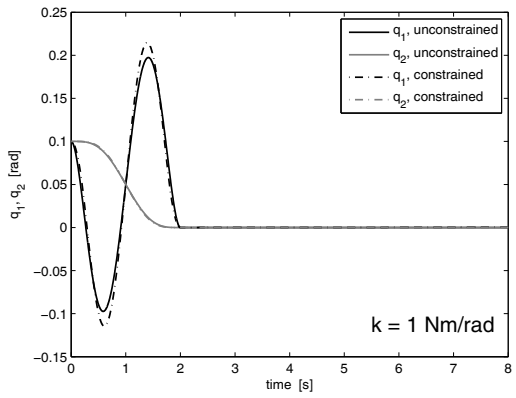

Fig. 10. Joint trajectory for the nominal case: constrained and unconstrained solution

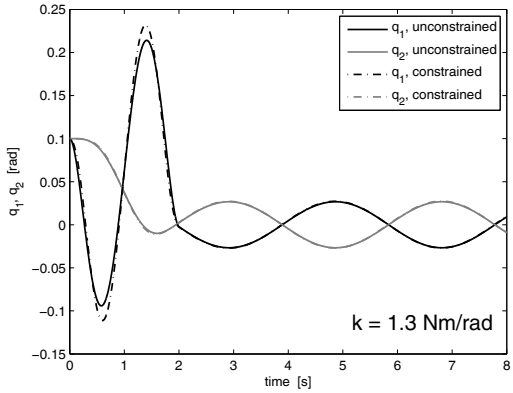

Fig. 11. Joint trajectory for the nominal case: constrained and unconstrained solution

leads to the results show in figure 11. The analysis of this plot highlights the presence of noticeable residual vibration after motion completion, i.e. after 2 seconds from the simulation starting point. The peak-to-peak amplitude of residual vibrations is equal to $0.056\ rad$, i.e. more than half of the prescribed mass displacement for the whole motion. A more complete evaluation of the residual vibration for the constrained and the unconstrained solution is shown in figure 12 in terms of residual energy of the system at time $t = t_f$. The residual energy E is evaluated as the sum of the kinetic energy T and the elastic energy U as:

$$E = T + U \tag{30}$$

in which the kinetic energy is simply:

$$T = \frac{1}{2}(J_1\omega_1^2 + J_2\omega_2^2) \tag{31}$$

while the elastic energy is:

$$\begin{aligned} U = \int_0^{\Delta q^*} F\Delta q d\Delta q &= \int_0^{\Delta q^*} (k\Delta q + k^3\Delta q) \\ &= k\left(\frac{1}{2}\Delta q^{*2} + \frac{1}{4}\Delta q^{*2}\right) \end{aligned} \tag{32}$$

The residual energy is used in this section as a measurement of the robustness of the outcome of the trajectory planning algorithm. Under nominal conditions,i.e. without any perturbations, the residual energy of the system must be equal to zero, since the prescribed right-side boundary condition is $\mathbf{x}(t_f) = \beta = [0, 0, 0, 0]^T$. Any deviation from this value can be measured through the use of the residual energy of the system, which can be seen as a norm of the vector $\mathbf{x}(t_d)$.

Figure 12 shows how the value of of the elastic constant k affects the value of residual energy after task completion. It can be seen in figure 12 that the residual energy is equal

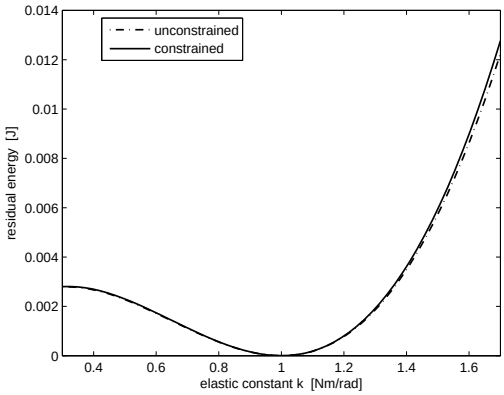

Fig. 12. Residual energy: unconstrained and constrained solutions, nominal trajectory with $k \in [0.3, 1.7]\ Nm/rad$

to zero only for $k = 1\ N/m$, and that the residual energy quickly grows with increasing and decreasing values of k. This applies with very similar trends for both the constrained and the unconstrained solutions. The following part of the paper will show how the use of sensitivity functions allows to improve the robustness of the computed trajectories with respect to variations of the elastic constant k.

As shown in the case of the simple mass-spring system, the robustness of the solution of the trajectory generation problem can be improved by imposing additional boundary condition on the sensitivity function in the optimization problem definition. Using the same procedure and applying it to the elastic joint case, the sensitivity equations can be computed as:

$$\begin{aligned}
&\frac{d}{dt}\left(\frac{\partial \omega_1}{\partial k}\right) = (q_2 - q_1) + (q_2 - q_1)^3 + \\
&\quad + k\left(\frac{\partial q_2}{\partial k} - \frac{\partial q_1}{\partial k}\right)^3 + 3k\left(\frac{\partial q_2}{\partial k} - \frac{\partial q_1}{\partial k}\right)(q_2 - q_1)^2; \\
&\frac{d}{dt}\left(\frac{\omega_2}{\partial k}\right) = -(q_2 - q_1) - (q_2 - q_1)^3 \\
&\quad - k\left(\frac{\partial q_2}{\partial k} - \frac{\partial q_1}{\partial k}\right)^3 - 3k\left(\frac{\partial q_2}{\partial k} - \frac{\partial q_1}{\partial k}\right)(q_2 - q_1)^2; \\
&\frac{d}{dt}\left(\frac{\partial q_1}{\partial k}\right) = \frac{\partial \omega_1}{\partial k}; \\
&\frac{d}{dt}\left(\frac{q_2}{\partial k}\right) = \frac{\partial \omega_2}{\partial k};
\end{aligned} \tag{33}$$

This choice of parametric uncertainty can be practically useful in all the cases in which the elastic constant of the flexible joint cannot be estimated with sufficient accuracy, or in the cases in which variations of the elastic constant are not described by the dynamic model used for trajectory planning. The Hamiltonian of the system is therefore:

$$\begin{aligned}
\mathcal{H} = {} & \lambda_3\omega_1 - \lambda_1\left(k(q_1 - q_2) - u + k(q_1 - q_2)^3\right) \\
& + \lambda_4\omega_2 + \lambda_7\frac{\partial \omega_1}{\partial k} + \lambda_8\frac{\partial \omega_2}{\partial k} \\
& - \lambda_5\left(q_1 - q_2 + (q_1 + q_2)^2 + k\left(\frac{\partial q_1}{\partial k} - \frac{\partial q_2}{\partial k}\right)\right) \\
& - 3\lambda_5 k(q_1 - q_2)^2\left(\frac{\partial q_1}{\partial k} - \frac{\partial q_2}{\partial k}\right) \\
& + \lambda_6\left(q_1 - q_2 + (q_1 + q_2)^2 + k\left(\frac{\partial q_1}{\partial k} - \frac{\partial q_2}{\partial k}\right)\right) \\
& + 3\lambda_6 k(q_1 - q_2)^2\left(\frac{\partial q_1}{\partial k} - \frac{\partial q_2}{\partial k}\right) \\
& + \lambda_2\left(k(q_1 - q_2) + k(q_1 - q_2)^3\right) + \frac{u^2}{2}
\end{aligned} \tag{34}$$

and the application of the condition of eq. (5) leads to the optimal control:

$$u^* = -\lambda_1 \tag{35}$$

Equations above refer to the unconstrained solution: hard limits on the control action can be achieved by direct substitution of λ_1 with the smoothing function defined in eq. (25). The complete formulation is here omitted due to the limited space availability. Boundary conditions are the same used for the nominal case, with the obvious addition of constraints on the sensitivity functions. The total execution time has been increased to $3.75\ s$ in order to produce a trajectory with the same peak torque as the nominal one. The control profile evaluated through the solution of the augmented TPBVP is shown in fig. 13: as in the previously shown nominal case (see fig. 8) the smoothing technique allows to precisely limit the control action in the range $[-2.5, 2.5]\ Nm$. The same solution shown in terms of joint positions is shown in figure 14: its accuracy is confirmed by the results available in figure 15, which shows the results of the feedforward application of the planned control profile. The absence of noticeable residual vibration highlights the accuracy of the solution when a nominal plant, therefore with $k = 1\ Nm$ is taken into account. The application of the same control profile to a plant with a stiffness values increased by 30% is reported in figure 16: the residual vibration has a peak-to-peak amplitude of 0.0161 rad, which is 3.4 times smaller than the same value obtained under the same conditions by the nominal trajectory, as visible from the comparison between figures 16 and 11.

A comparison in terms of residual energy between the nominal and robust solutions, with and without the application of constraints, is shown in figure 17. The figure shows how a change in the value of the elastic constant k for a $\pm 30\%$ variation influences the residual energy after motion completion. The analysis of the data presented in

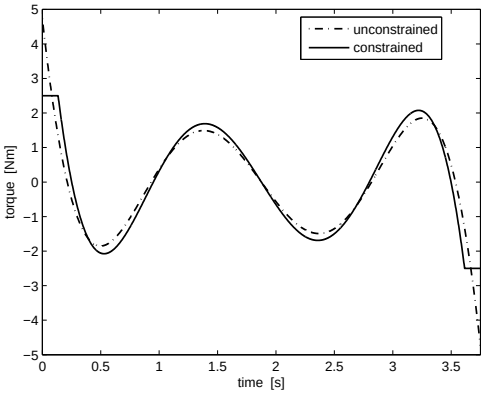

Fig. 13. Robust solution: torque for unconstrained and constrained solutions

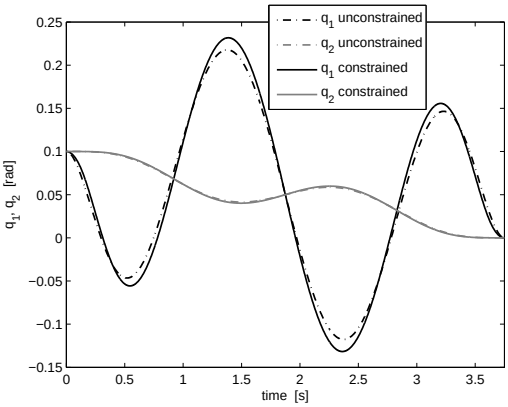

Fig. 14. Planned trajectory: robust solutions

this graph allows to conclude that, for the case under consideration, the inclusion of robustness conditions allows to significantly reduce the sensitivity of the plant to parametric mismatches, and that the inclusion of hard constraints on the actuator effort has a very limited effect on the robustness properties of the planned trajectory.

V. Conclusions

In this paper the problem of generating model-based robust trajectories for nonlinear mechatronic systems is dealt with. The work proposed a method based on the use of sensitivity function which allows to improve the robustness to parametric mismatches to augment the classic approach based on the solution of a two-point boundary value problem. Also the problem of including constraints is dealt with, using an accurate smoothing technique. The effectiveness of the approach is tested on two benchmark problem: a nonlinear mass-spring system and a nonlinear flexible joint manipulator. Results highlight that the proposed approach can lead to a sensible improvement to parametric mismatches of the planning trajectory, and that constraints can be included with accuracy without affecting the parametric robustness

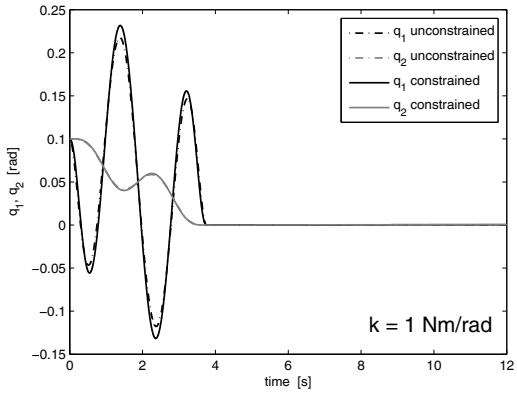

Fig. 15. Joint trajectories for the nominal case: robust solutions

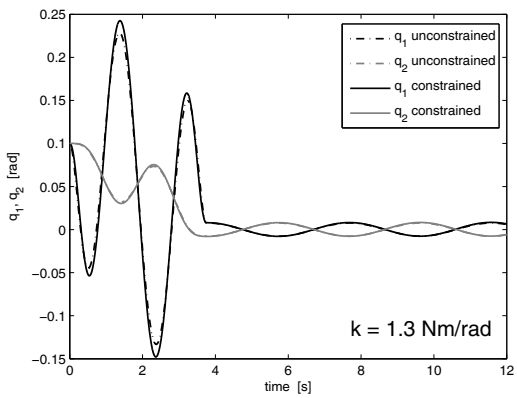

Fig. 16. Joint trajectories for the perturbed plant ($k = 1.3\ Nm/rad$): robust solutions

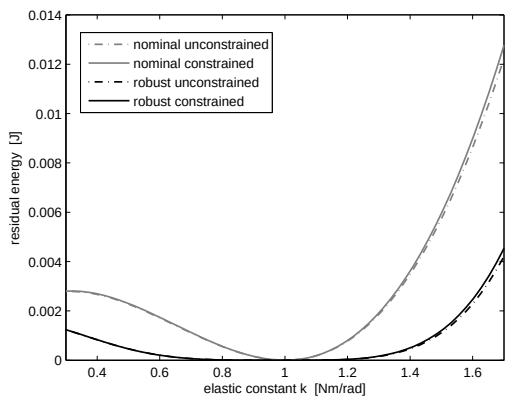

Fig. 17. Comparison of the residual energy between nominal, nominal constrained, robust and robust constrained solutions

of the solution.

References

[1] A. De Luca, G. Di Giovanni, Rest-to-rest motion of a two-link robot with a flexible forearm, in: Advanced Intelligent Mechatronics, 2001. Proceedings. 2001 IEEE/ASME International Conference on, Vol. 2, IEEE, 2001, pp. 929–935.

[2] P. Gallina, A. Trevisani, Synthesis and experimental validation of a delayed reference controller for active vibration suppression in mechanical systems, Journal of applied mechanics 72 (4) (2005) 623–627.

[3] P. Boscariol, V. Zanotto, Design of a controller for trajectory tracking for compliant mechanisms with effective vibration suppression, Robotica 30 (01) (2012) 15–29.

[4] S. Moberg, E. Wernholt, S. Hanssen, T. Brogårdh, Modeling and parameter estimation of robot manipulators using extended flexible joint models, Journal of Dynamic Systems, Measurement, and Control 136 (3) (2014) 031005.

[5] R. Vidoni, A. Gasparetto, M. Giovagnoni, Design and implementation of an erls-based 3-d dynamic formulation for flexible-link robots, Robotics and Computer-Integrated Manufacturing 29 (2) (2013) 273–282.

[6] R. Vidoni, A. Gasparetto, M. Giovagnoni, A method for modeling of three-dimensional flexible mechanisms based on an equivalent rigid-link system, Journal of Vibration and Control 20 (4) (2014) 483–500.

[7] A. A. Ata, Optimal trajectory planning of manipulators: a review, Journal of Engineering Science and Technology 2 (1) (2007) 32–54.

[8] A. Gasparetto, P. Boscariol, A. Lanzutti, R. Vidoni, Trajectory planning in robotics, Mathematics in Computer Science (2012) 1–11.

[9] P. Boscariol, A. Gasparetto, Model-based trajectory planning for flexible-link mechanisms with bounded jerk, Robotics and Computer-Integrated Manufacturing 29 (2013) 90–99.

[10] P. Boscariol, A. Gasparetto, R. Vidoni, A. Romano, A model-based trajectory planning approach for flexible-link mechanisms, in: Mechatronics (ICM), 2013 IEEE International Conference on, IEEE, 2013, pp. 219–224.

[11] R. Caracciolo, D. Richiedei, A. Trevisani, Experimental validation of a model-based robust controller for multi-body mechanisms with flexible links, Multibody System Dynamics 20 (2) (2008) 129–145.

[12] M. Boryga, A. Graboś, Planning of manipulator motion trajectory with higher-degree polynomials use, Mechanism and machine theory 44 (7) (2009) 1400–1419.

[13] P. Boscariol, A. Gasparetto, R. Vidoni, Jerk-continuous trajectories for cyclic tasks, in: ASME 2012 International Design Engineering Technical Conferences and Computers and Information in Engineering Conference, American Society of Mechanical Engineers, 2012, pp. 1277–1286.

[14] C. Louembet, F. Cazaurang, A. Zolghadri, Motion planning for flat systems using positive b-splines: An lmi approach, Automatica 46 (8) (2010) 1305–1309.

[15] P. Boscariol, A. Gasparetto, R. Vidoni, Planning continuous-jerk trajectories for industrial manipulators, in: ASME 2012 11th Biennial Conference on Engineering Systems Design and Analysis, American Society of Mechanical Engineers, 2012, pp. 127–136.

[16] D. Balkcom, M. Mason, Time optimal trajectories for bounded velocity differential drive vehicles, The International Journal of Robotics Research 21 (3) (2002) 199–217.

[17] O. Dahl, Path constrained motion optimization for rigid and flexible joint robots, in: International Conference on Robotics and Automation, Vol. 2, IEEE, 1993, pp. 223–229.

[18] M. Korayem, H. R. Nohooji, A. Nikoobin, Optimal motion generating of nonholonomic manipulators with elastic revolute joints in generalized point-to-point task, International journal of advanced design and manufacturing technology 3 (2) (2010) 1–9.

[19] A. Abe, Trajectory planning for residual vibration suppression of a two-link rigid-flexible manipulator considering large deformation, Mechanism and Machine Theory 44 (9) (2009) 1627–1639.

[20] M. Korayem, A. Nikoobin, V. Azimirad, Trajectory optimization of flexible link manipulators in point-to-point motion, Robotica 27 (6) (2009) 825–840.

[21] D. Gallardo, O. Colomina, F. Flórez, R. Rizo, A genetic algorithm for robust motion planning, Tasks and Methods in Applied Artificial Intelligence (1998) 115–121.

[22] K. G. Shin, N. D. McKay, Robust trajectory planning for robotic manipulators under payload uncertainties, Automatic Control, IEEE Transactions on 32 (12) (1987) 1044–1054.

[23] B. Houska, Robust optimization of dynamic systems, Ph.D. thesis, PhD thesis, Katholieke Universiteit Leuven, 2011.(ISBN: 978-94-6018-394-2) (2011).

[24] T. Singh, Optimal reference shaping for dynamical systems: theory and applications, CRC PressI Llc, 2010.

[25] T. A. Hindle, T. Singh, Desensitized minimum power/jerk control profiles for rest-to-rest maneuvers, in: American Control Conference, 2000. Proceedings of the 2000, Vol. 5, IEEE, 2000, pp. 3064–3068.

[26] R. Kased, T. Singh, Rest-to-rest motion of an experimental flexible structure subject to friction: Linear programming approach, in: AIAA Guidance, Navigation and Control Conference, San Francisco, CA, 2005.

[27] L. Pontryagin, R. Gamkrelidze, The mathematical theory of optimal processes, Vol. 4, CRC, 1986.

[28] L. Shampine, I. Gladwell, S. Thompson, Solving ODEs with MATLAB, Cambridge University Press, 2003.

[29] R. W. Holsapple, A modified simple shooting method for solving two-point boundary value problems.

[30] G. Boschetti, R. Caracciolo, D. Richiedei, A. Trevisani, A non-time based controller for load swing damping and path-tracking in robotic cranes, Journal of Intelligent & Robotic Systems (2014) 1–17.

[31] S. Moberg, On modeling and control of flexible manipulators, Ph.D. thesis, Department of Electrical Engineering, Linkping University, Sweden (2007).

[32] P. Axelsson, Evaluation of six different sensor fusion methods for an industrial robot using experimental data, in: 10th International IFAC Symposium on Robot Control, Dubrovnik, Croatia, 2012.

[33] P. Axelsson, M. Norrlöf, E. Wernholt, F. Gustafsson, Extended kalman filter applied to industrial manipulators, in: Proceedings of Reglermöte 2010, Lund, Sweden, 2010.

[34] S. Avvakumov, Y. N. Kiselev, Boundary value problem for ordinary differential equations with applications to optimal control, Spectral and Evolution Problems 2000 10.